ORBITAL MOTION EQUATIONS WITH DYNAMIC MODELS*

Douglas H. May†

Kepler's equation for time as a function of position in an elliptic orbit is of primary importance in predicting any satellite's orbital position. His approach provides the foundation for the derivation of time-position equations for the other orbits as well. In this paper, fundamentals of classical mechanics are applied to analyze two-body trajectories, and results of the method presented are compared with the classical equations. Power, energy, and time-displacement equations are derived by integration beginning with a summation of the forces acting. In each case – elliptic, parabolic, and hyperbolic – the derivation produces new models based on circles. The models presented provide displacement and velocity vector relationships for each orbit type. Elliptic and hyperbolic orbit equations are expressed as trigonometric functions of conformance angles that result naturally from the integration steps. All the models can be constructed in a coordinate system that is fixed relative to the radius vector. Equations and models for rectilinear trajectories are derived for each special case of the corresponding general orbit. Rectilinear equations and dynamic models complete the family of two-body trajectories and provide continuity in the mathematic relationships for all orbits.

NOMENCLATURE

E = eccentric anomaly, elliptic orbit conformance angle
H = hyperbolic anomaly
$\mathcal{E}$ = total specific mechanical energy
a = semi-major axis
e = eccentricity
h = specific angular momentum
p = semi-latus rectum or semi parameter
r = radius, radial distance
t = time
η = hyperbolic orbit conformance angle
μ = gravitational constant
θ = true anomaly

---

* Originally presented as Paper AAS 05-354, "Orbital Motion Equations With Dynamic Models," at the AAS/AIAA Astrodynamics Specialist Conference, Lake Tahoe, CA, August 2005, and published in *Astrodynamics 2005*, Advances in the Astronautical Sciences, Vol. 123, Univelt, Inc., beginning on p. 1611. Posted with permission of the American Astronautical Society. This version contains minor revisions: E replaces ε for the eccentric anomaly, and equation and figure numbering have been corrected. Not for commercial use.

† Douglas H. May, PE, faculty member of Embry-Riddle Aeronautical University, 5260 E. Granite St., Davis-Monthan AFB, AZ 85707-3009. E-mail: dougmay@gmail.com.

INTRODUCTION

Kepler recognized that planets moved in elliptic orbits with the radius vector sweeping out equal areas in equal times. By circumscribing a circle about the ellipse, he was able to derive the classic elliptic time-displacement equation. Similar geometric constructions for parabolic and hyperbolic orbits give their time-displacement equations. The position of satellites, both natural and artificial, is predicted by equations based on Kepler's method.

Equations of orbital dynamics can also be derived from basic principles of classical mechanics through a sequence of integration steps without constructing area relationships. This integration approach is central to this paper and gives results that can be checked with classical equations. It also produces models that are helpful in describing the full range of motion for each orbit type. For example, each elliptic, parabolic, and hyperbolic type of trajectory has a special case of rectilinear motion. The rectilinear equations fill in what otherwise are discontinuities in the family of two-body orbital trajectories. The models derived with the integration approach represent the linear trajectories, but since no area is swept out by the radius vector, the classical approach has difficulty including them. The equations relate to conic sections, and models for the rectilinear cases include the singularity that is evident at the apex of the cone. The basic principles of the method were documented in Reference 1. This paper expands on those principles.

The models in this paper were developed by the author as an aid to visualize the conformance angles that are found with the method. No other physical significance is claimed but realizing that orbital motion can be represented in a coordinate system other than the perifocal system has merit. The models presented in this paper and the derivation steps make it clear that the radial component of motion and component normal to the radius can be represented as separate quantities. The classical coordinate system that is fixed relative to the distant stars serves us well. However, we can gain additional understanding of orbital motion with other coordinate systems.

KEPLER'S APPROACH

Kepler's second law, the radius vector sweeping equal areas in equal times, has a parallel principle in mechanics, angular momentum is conserved in the torque-free motion of two-body orbits. The magnitude of angular momentum, h, is written[2]

$$h = r^2\dot{\theta} \,. \tag{1}$$

Radial displacement, r, is the distance between body centers and θ is the true anomaly. This equation applies to each type of orbit.

The derivation of the trajectory equation gives a vector relationship. In the derivation we see that all two-body orbits can be described with the general polar coordinate equation for conic sections. This equation gives the radius as a function of the semi parameter, p, eccentricity, e, and θ. It is written as[3]

$$r = \frac{p}{1 + e\cos\theta} \,. \tag{2}$$

The same derivation produces the value for h in all orbits in terms of the gravitational constant, μ, and p:

$$h = \sqrt{\mu p} \,. \tag{3}$$

Kepler gave us a geometric relationship between the elliptic orbit and a circumscribed auxiliary circle with a radius of a, the semi-major axis, that quantifies the area increase or decrease with time according to

his law. His construction and the eccentric anomaly, E, are shown in Figure 1. The resulting equation gives time-displacement as

$$\sqrt{\frac{\mu}{a}}\,t = aE - ae\sin E \tag{4}$$

when time is zero at periapsis.

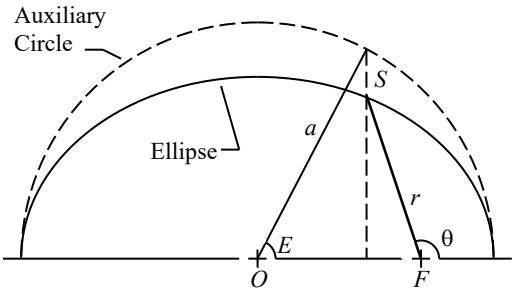

Figure 1 Geometry of Kepler's Equation.

Area relationships for parabolic and hyperbolic orbits allow us to write time-displacement equations for those cases also. However, the parabolic orbit with $e = 1$ has a unique integrated solution with Eq. (2) substituted into Eq. (1) and variable separation. The hyperbolic diagram applies a special case and defines the hyperbolic anomaly to derive an equation involving a hyperbolic function. The special case is the equilateral hyperbola in which the eccentricity is equal to the square root of two. This is analogous to the auxiliary circle for the ellipse.[4]

FUNDAMENTAL EQUATIONS OF ORBITAL DYNAMICS

Figure 2 shows the forces acting in a general case of a satellite moving in the gravitational field of a parent body. As previously stated, this simple mechanical system is free of torque, so each of the forces acts along the radius vector. Gravity acts toward the center of mass of the parent body, and a centrifugal force associated with the rotational component of motion acts in the positive r direction. In accordance with Newton's second law, the satellite will experience an acceleration that is equal in magnitude to the algebraic sum of the other two forces. It can be in either direction. The equivalency principle allows us to add these forces. Though the quantities are vectors, they can be added algebraically because they are always aligned. The mass of the satellite is unity, a conventional assumption which is valid because satellite mass applies to each force and cancels.

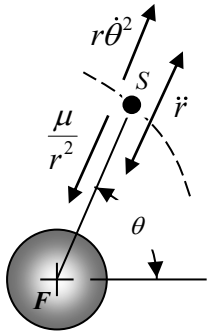

Figure 2 Forces on a Satellite.

Write the force summation equation matching Figure 2 as

$$\ddot{r} = r\dot{\theta}^2 - \frac{\mu}{r^2} \cdot \tag{5}$$

In this two-body system no work crosses the boundaries. Within the system, power associated with a force is expressed as the rate at which the force does work. Mathematically this is the dot product of the force vector and the velocity vector, $\vec{\dot{r}}$. Algebraic multiplication satisfies the vector dot product because of the radial alignment. A power equation is then found by multiplying each term in Eq. (5) by $\dot{r}$ and is written

$$\dot{r}\ddot{r} = r\dot{r}\dot{\theta}^2 - \frac{\mu\dot{r}}{r^2}. \tag{6}$$

Power and the energy terms in the equations that follow are scalar quantities. Vector notation is not shown in succeeding derivations. The time-displacement equations are derived by integration, and Ref. 6 is the source for integrals and other formulas.

Combining Eq. (1) and Eq. (3) and substituting into Eq. (5),

$$\dot{r}\ddot{r} - \frac{\mu p\dot{r}}{r^3} + \frac{\mu\dot{r}}{r^2} = 0 \tag{7}$$

Integrating power with respect to time gives energy change or work performed,

$$\frac{\dot{r}^2}{2} + \frac{up}{2r^2} - \frac{\mu}{r} = \mathcal{E} \tag{8}$$

Equation (8) is the familiar conservation-of-energy equation for general orbital motion. The constant $\mathcal{E}$ represents the total specific mechanical energy for each trajectory type.

RECTILINEAR TRAJECTORIES

Kepler's laws, Eq. (1) and Eq. (2) address only those trajectories with a rotational component, and the literature often implies that all two-body motion has this component. However, the rotational term is zero for rectilinear motion. Trajectories in which a satellite moves directly toward or away from its parent body are real. This special case will be analyzed for elliptic, parabolic and hyperbolic motion.

Equation (8) applies to rectilinear trajectories when the rotational term is eliminated, and

$$\ddot{r} = \frac{\mu}{r^2} \tag{9}$$

The power relationship then becomes

$$\dot{r}\ddot{r} = -\frac{\mu\dot{r}}{r^2} \tag{10}$$

Integrating with respect to time gives conservation of energy for non-rotational motion, a special case of Eq. (8),

$$\frac{\dot{r}^2}{2} - \frac{\mu}{r} = \mathcal{E} \tag{11}$$

Eccentricity for any conic section may be expressed in terms of total energy and angular momentum, [2]

$$e = \sqrt{1 + \frac{2\mathcal{E}h^2}{\mu^2}} \tag{12}$$

A parabolic orbit has an eccentricity of one. The eccentricities of elliptic and hyperbolic trajectories with non-zero values of $\mathcal{E}$ are also one when $\boldsymbol{h}$ is zero and the motion is linear.

An integration approach helps explain the discontinuity that we see between the types of orbits when we take the classical approach.[2] Equations for elliptic paths are continuous for all values of *e* less than *or* equal to one. The linear parabolic equation can then be shown to be the limiting case as total energy approaches zero. The same continuity statement can be made for hyperbolic paths.

As each type of orbit is analyzed, Eq. (12) will be included in the analysis with the appropriate value of $\mathcal{E}$. In each case the linear trajectory will be continuous with the general orbit equations.

ELLIPSE

Equation (2) describes an ellipse in polar coordinates when the value of *e* is between zero and one, zero being the special case of a circle. A linear trajectory with total energy in the elliptic range and an eccentricity of one will also be analyzed. The general elliptic orbit is analyzed first.

General

Equation (8) represents elliptic orbits when the total energy, $\mathcal{E}$, is equal to $-\mu/2a$, eccentricity is one or less, and $\boldsymbol{h}$ and *p* have non-zero values.[4] Substituting and rearranging, we write

$$\dot{r}^2 = \left(\frac{\mu}{a}\right)\frac{2ar - r^2 - ap}{r^2} \quad . \tag{13}$$

This may be rewritten with $p = a(1 - e^2)$ as, [4]

$$\dot{r}^2 = \left(\frac{\mu}{a}\right)\frac{a^2e^2 - (a-r)^2}{r^2} \quad . \tag{14}$$

Rearrange, take the square root, and separate variables to write the following integral equation (positive root):

$$\sqrt{\frac{\mu}{a}}\int dt = \int \frac{r\,dr}{\sqrt{a^2e^2 - (a-r)^2}} \tag{15}$$

Integrate, and we can write

$$\sqrt{\frac{\mu}{a}}\,t = -\sqrt{a^2e^2 - (a-r)^2} \; - a\sin^{-1}\left(\frac{a-r}{ae}\right) + C \tag{16}$$

To be consistent with Kepler's equation, let $t = 0$ at periapsis, and $C = a\pi/2$. Then define the angle variable that is the $\sin^{-1}$ angle in Eq. (16) as α, and Kepler's E is identified as the complement of that angle,

$$E = \frac{\pi}{2} - \alpha = \cos^{-1}\left(\frac{a-r}{ae}\right) \tag{17}$$

Equation (17) gives the relationship for r as

$$r = a - ae\cos E \cdot \tag{18}$$

Equation (16) now reduces to

$$\sqrt{\frac{\mu}{a}}\,t = aE - ae\sin E \tag{19}$$

if time is zero at periapsis.

Figure 3 shows a model that conforms to Eqs. (17) and (18). Constant lines in this model are dotted, and subsequent models will apply this same distinction.

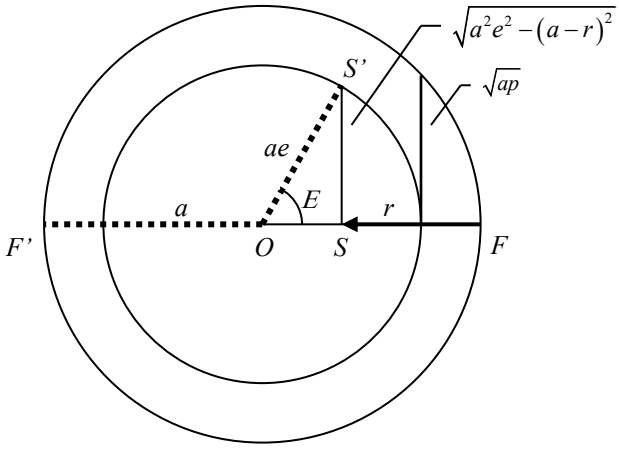

Figure 3 General Elliptic Orbit Model.

Linear Elliptic Motion

Rectilinear motion for a path with total energy in the elliptic range is a special case of the motion described above. Figure 4 represents linear elliptic trajectories when the circles in Figure 3 coincide.

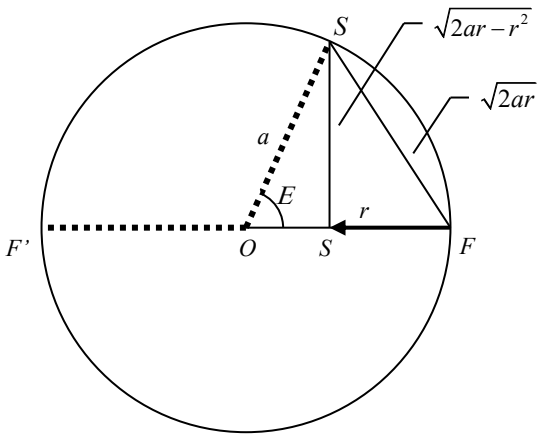

Figure 4 Linear Elliptic Trajectory Model.

The derivation of motion equations is the same as the general case with e equal to one ($p = 0$) in the steps from Eqs. (12-19). Continuity between the general model and the linear model is not as evident with the classical approach because there is no sweeping of area by the radius vector. However, one can see that the model above and Kepler's model coincide in the linear case, but this gets little attention in the literature. Equation (19) represents linear elliptic motion when $e = 1$.

Note that this formulation uses the boundary condition $t = 0$ at $r = 0$, which makes the constant of integration equal to zero. Although $r = 0$ is a mathematical singularity and would normally be unsuitable as a boundary condition, the angular displacement relationship makes it acceptable in this context. In practical applications, Eq. (19) is evaluated at two states and subtracted, eliminating the constant of integration.

Dynamic Models

The equations and models derived above for elliptic trajectories allow us to model the energy conservation equation. Lines represent the square root of twice the energy magnitude in each term. The models are referred to as dynamic models to distinguish them from the displacement models.

Differentiate Eq. (19) with respect to time to give

$$\sqrt{\frac{\mu}{a}} = a\left(1 - e\cos E\right)\dot{E} \tag{20}$$

or

$$r\dot{E} = \sqrt{\frac{\mu}{a}} \tag{21}$$

Then differentiate Eq. (18) with $e = 1$ with respect to time to give

$$ae\sin E\,\dot{E} = \dot{r} \tag{22}$$

or

$$\sqrt{a^2e^2 - \left(a - r\right)^2}\,\dot{E} = \dot{r} \tag{23}$$

We can see by rearranging Eq. (21) that

$$\sqrt{2ar}\,\dot{E} = \sqrt{\frac{2\mu}{r}}\,. \tag{24}$$

A dynamic linear elliptic model is developed first to show the relationships with a reduced set of variables. Equations (20) through (24) with the value $e = 1$ show that multiplying lines in the model in Figure 4 by $\dot{E}$ gives significant velocity terms. A dynamic linear elliptic model is shown in Figure 5. Squaring the sides of the FSS' triangle gives conservation of energy. The Pythagorean theorem gives the proper relationship when it is written as

$$\frac{2\mu}{r} = \dot{r}^2 + \frac{\mu}{a}\,. \tag{25}$$

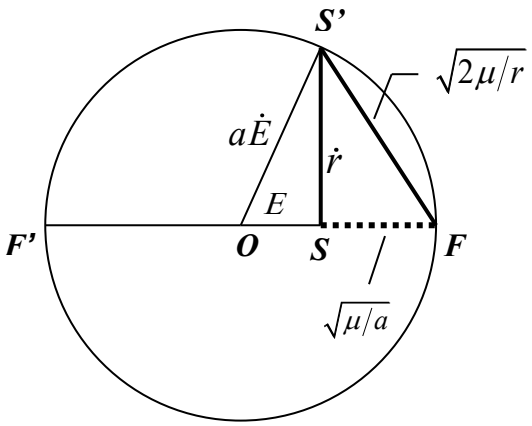

Figure 5 Dynamic Linear Elliptic Model.

The circle in this dynamic model and all lines except the dotted line *FS* vary with time. The circle expands to infinity as E goes to zero, another phenomenon associated with the boundary condition.

General Case

To extend the dynamic model to the general case we must include the energy term associated with rotational motion. The energy equation may be written

$$\frac{2\mu}{r} = \dot{r}^2 + \frac{\mu p}{r^2} + \frac{\mu}{a} \tag{26}$$

Equations (23-26) apply with e between zero and one. We find velocity normal to r by combining Eqs. (1) and (21),

$$r\dot{\theta} = \sqrt{\frac{\mu p}{r^2}} = \sqrt{ap}\,\dot{E} \tag{27}$$

General elliptic motion can be modeled much like the linear case. We can again see that multiplying lines in Figure 3 by $\dot{E}$ gives the appropriate vectors. However, this model must be three dimensional to represent the four energy terms in Eq. (26). The rotational vector is any line equal to $\sqrt{ap}$ in the model multiplied by $\dot{E}$. If this line is selected perpendicular to the paper, a solid is found with the sides giving the proper relationship. The sum of the squares of the sides equals twice the potential energy as in Eq. (26) if the model is constructed

as shown in Figure 6. The solid that matches the equation is defined by *FS*, *S'*, and *S"*. Only the dotted line *FS* remains constant in this model.

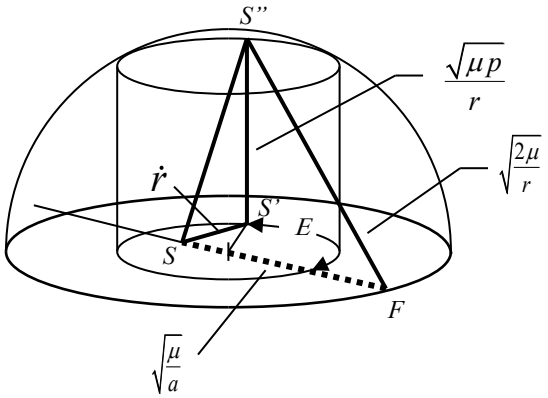

Figure 6 Dynamic Elliptic Orbit Model.

PARABOLA

Algebraic time-displacement equations for parabolic orbits are found by substituting Eq. (2) into Eq. (1), separating variables and integrating. However, the method presented in this paper serves to produce the same result. It is shown in this section just for comparison. The equations for this motion have a total energy of zero and an eccentricity of one. [2]

General

A general parabolic orbit has non-zero values of $\boldsymbol{h}$ and p. It is unique in that velocity approaches zero as r approaches infinity, and the radius at periapsis is $p/2$. Substitute zero for $\boldsymbol{\mathcal{E}}$ in Eq. (8) and rearrange the result to give

$$\dot{r}^2 = \mu\left(\frac{2r-p}{r^2}\right) . \tag{28}$$

Rearrange again, separate variables and select the positive root to write the integral equation

$$\sqrt{\mu}\int dt = \int \frac{rdr}{\sqrt{2r-p}} . \tag{29}$$

Integrate and write

$$\sqrt{\mu}\,t = \frac{r+p}{3}\sqrt{2r-p} + C . \tag{30}$$

This relationship is simplified if $\boldsymbol{t} = 0$ at periapsis and $C = 0$. Square both sides and rearrange and write the time-displacement relationship,

$$r^3 + \frac{3p}{2}r^2 - \left(\frac{p^3 + 9\mu t^2}{2}\right) = 0 . \tag{31}$$

An alternate well documented time-displacement equation may be written in terms of θ by substituting

$$r = \frac{p}{1+\cos\theta} = \frac{p}{2}\sec^2 \theta/2 \tag{32}$$

into Eq. (31). With the same boundary condition as above, write[4]

$$\tan^3 \theta/2 + 3\tan\theta/2 - 6\sqrt{\frac{\mu}{p^3}}\,t = 0 \tag{33}$$

Parabolic orbital position as a function of time is found as a real cubic solution for Eq. (31) or Eq. (33). In terms of radial displacement, the equation is

$$r = \frac{p}{2}\left[\sqrt[3]{1+\frac{18\mu t^2}{p^3}+\sqrt{\left(1+\frac{18\mu t^2}{p^3}\right)^2-1}} + \sqrt[3]{1+\frac{18\mu t^2}{p^3}-\sqrt{\left(1+\frac{18\mu t^2}{p^3}\right)^2-1}} - 1\right] \tag{34}$$

and in terms of angular displacement, it is

$$\tan\frac{\theta}{2} = \sqrt[3]{3\sqrt{\frac{\mu}{p^3}}\,t+\sqrt{1+\frac{9\mu t^2}{p^3}}} - \sqrt[3]{3\sqrt{\frac{\mu}{p^3}}\,t-\sqrt{1+\frac{9\mu t^2}{p^3}}} \tag{35}$$

Motion may be modeled relative to a circle which presents a clear representation of a parabolic orbit and gives a means of developing another model displaying kinetic and potential energies. A variation of the classic model is shown in Figure 7. Satellite motion is modeled as a parabola just as in the classic model with the true anomaly and radius relationship. The radius of the circle varies from $p/2$ to infinity while the magnitude of p (dotted line) remains constant.

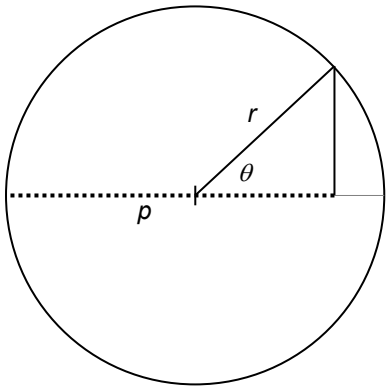

Figure 7 General Parabolic Orbit Model.

Linear Parabolic Dynamics

If motion is generally parabolic but rectilinear, we have Eq. (11) with $\mathcal{E} = 0$. Take the square root and write

$$\dot{r} = \pm\sqrt{\frac{2\mu}{r}} \tag{36}$$

Choose the positive root in Eq. (36), separate variables and integrate to give

$$\pm\sqrt{2\mu}\,t = \tfrac{2}{3} r^{3/2} + C \tag{37}$$

Evaluate the constant by letting $t = 0$ when $r = r_0$, and the time-displacement equation becomes

$$\pm\sqrt{\mu}\,t = \tfrac{\sqrt{2}}{3}\left(r^{3/2} - r_0^{3/2}\right) \tag{38}$$

Equation (38) can be rewritten to express an angular rate as a function of time by dividing by $r_0^{3/2}$,

$$\frac{\sqrt{2}}{3} \pm \sqrt{\frac{\mu}{r_0^3}}\,t = \frac{\sqrt{2}}{3}\left(\frac{r}{r_0}\right)^{3/2} \tag{39}$$

The first term in Eq. (39) determines the angle at which the path begins in the polar coordinate system. The curve is shown in Figure 8 with a uniform increase in the angle with time. Note that r goes to zero at an angular deflection of $-\sqrt{2}/3$ radians. As in other two-body problems, we are interested in an equation for the difference between two points on the path. This is obtained by subtracting Eq. (39) for one state from its value for another. The constant drops out.

Three-dimensional models are indicated in this case if both sides of Eq. (39) are squared. The significance of this is not pursued in this paper.

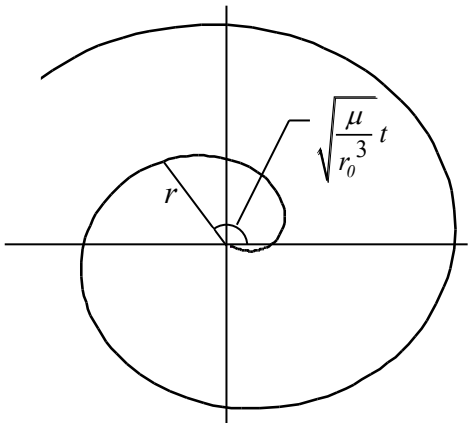

Figure 8 A Linear Parabolic Trajectory Model

Dynamic Models

The dynamic model that represents parabolic trajectories must satisfy the conservation of energy equation written as

$$\frac{2\mu}{r} = \dot{r}^2 + \frac{\mu p}{r^2} \cdot \tag{40}$$

We begin to develop this model by finding the velocity in the radial direction which is the time derivative of Eq. (32),

$$\dot{r} = p \sec^2 \frac{\theta}{2} \tan \frac{\theta}{2} \frac{\dot{\theta}}{2} \cdot \tag{41}$$

Substitute Eq. (32) into Eq. (41) to write

$$\dot{r} = 2r \tan \frac{\theta}{2} \frac{\dot{\theta}}{2} \cdot \tag{42}$$

By inspection, the velocity components that satisfy the conservation of energy equation are obtained by multiplying lines in Figure 7 by $\dot{\theta}/2$. The diameter of the inner circle, $2r$ times $\dot{\theta}/2$, gives the velocity normal to r in a dynamic model,

$$r\dot{\theta} = \frac{\sqrt{\mu p}}{r} \cdot \tag{43}$$

Square the terms and add Eqs. (42) and (43) to write

$$\frac{2\mu}{r} = \dot{r}^2 + \frac{\mu p}{r^2} = 4r^2 \left(1 + \tan^2 \frac{\theta}{2}\right)\left(\frac{\dot{\theta}}{2}\right)^2 = 4r^2 \sec^2 \frac{\theta}{2}\left(\frac{\dot{\theta}}{2}\right)^2 \cdot \tag{44}$$

We can then construct the model as shown in Figure 9, and the *ABC* triangle satisfies conservation of energy as written in Eq. (40).

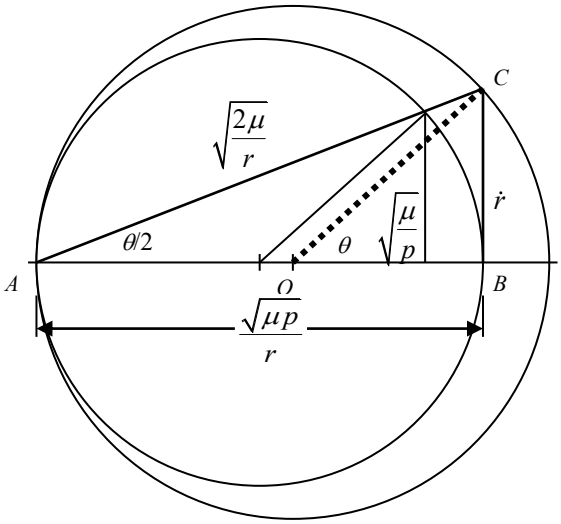

Figure 9 The Dynamic Parabolic Model

The radius of the outer circle in Figure 9 is

$$\overline{OC} = 2r \sec^2 \frac{\theta}{2} \frac{\dot{\theta}}{2} \cdot \tag{45}$$

Substitute Eq. (32) into this equation gives

$$\overline{OC} = \frac{2r^2}{p}\frac{\dot{\theta}}{2} = \sqrt{\frac{\mu}{p}} \tag{46}$$

and the radius of the outer circle (dotted line) remains constant and equal to $\sqrt{\mu / p}$ for the full range of motion.

A dynamic model for the linear case must represent the relationship in Eq. (40) with $p = 0$. Terms that have velocity units and satisfy the vis viva equation are related as shown in Figure 10.

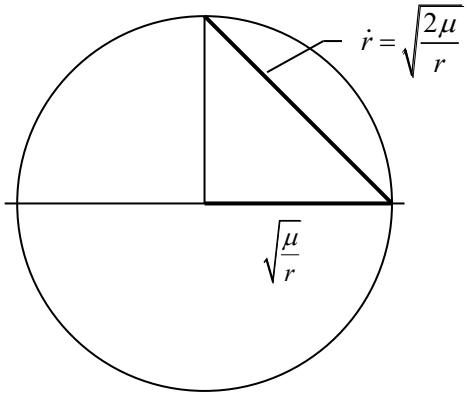

Figure 10 Linear Parabolic Dynamic Model

HYPERBOLA

The approach presented for deriving motion equations shows the greatest difference in results from the classical method for the hyperbolic trajectory. Instead of hyperbolic functions, the relationships are represented by trigonometric equations. The linear trajectory with total energy in the hyperbolic range and eccentricity equal to one will be analyzed as a special case. The general hyperbolic orbit is analyzed first.

General

A satellite follows a hyperbolic trajectory when its eccentricity is greater than one and h and p have non-zero values. Eq. (8) represents hyperbolic orbits when the total energy is positive and equal to $\mu /2a$.[4] Substitute this value and rearrange Eq. (8) to write

$$\dot{r}^2 = \left(\frac{\mu}{a}\right)\frac{2ar + r^2 - ap}{r^2} \cdot \tag{47}$$

Substitute $p = a(e^2 - 1)$ into Eq. (47) and rearrange this equation to write

$$\dot{r}^2 = \left(\frac{\mu}{a}\right)\frac{(a+r)^2 - a^2e^2}{r^2} \quad \cdot \tag{48}$$

Rearrange again and separate variables to give the following integral equation:

$$\sqrt{\frac{\mu}{a}}\int dt = \int \frac{r\,dr}{\sqrt{(a+r)^2 - a^2e^2}} \tag{49}$$

Integrate this expression to write

$$\sqrt{\frac{\mu}{a}}t = ea\frac{\sqrt{(a+r)^2 - a^2e^2}}{ae} - a\ln\left(a + r + \sqrt{(a+r)^2 - a^2e^2}\right) + C \tag{50}$$

Letting $t = 0$ at periapsis allows us to evaluate the constant and write

$$\sqrt{\frac{\mu}{a}}t = ae\sqrt{\left(\frac{a+r}{ae}\right)^2 - 1} - a\ln\left(\frac{a+r}{ae} + \sqrt{\left(\frac{a+r}{ae}\right)^2 - 1}\right) \tag{51}$$

which is written in this form to highlight the $(a + r)/ae$ term. With the substitution of the simplifying variable

$$\eta = \cos^{-1}\frac{ae}{a+r} = \sec^{-1}\frac{a+r}{ae}, \tag{52}$$

we have radial displacement expressed as

$$r = ae\sec\eta - a \cdot \tag{53}$$

A model that conforms to the equations above is shown in Figure 11.

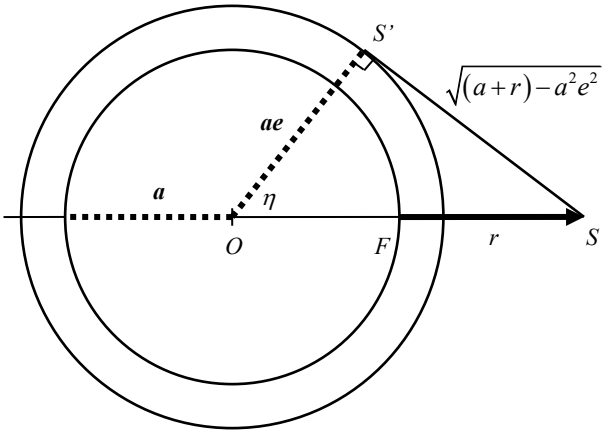

Figure 11 General Hyperbolic Orbit Model.

Substitute Eq. (53) into Eq. (51) and write

$$\sqrt{\frac{\mu}{a}}t = ae\tan\eta - a\ln\left(\sec\eta + \tan\eta\right) + C \tag{54}$$

This also may be expressed as

$$\sqrt{\frac{\mu}{a}}t = ae\tan\eta - a\ln\left[\tan\left(\frac{\pi}{4} + \frac{\eta}{2}\right)\right] + C \tag{54a}$$

The constant of integration is zero if $t = 0$ at periapsis.

Linear Hyperbolic Motion

Rectilinear motion for a trajectory with total energy in the hyperbolic range is a special case of the motion described above. The term involving rotational motion in Eq. (8) drops out, and the development of motion equations parallels the steps for general hyperbolic motion. Resulting equations are the same as the general equations above with eccentricity equal to one. Figure 12 represents linear hyperbolic trajectory with the two coincident circles

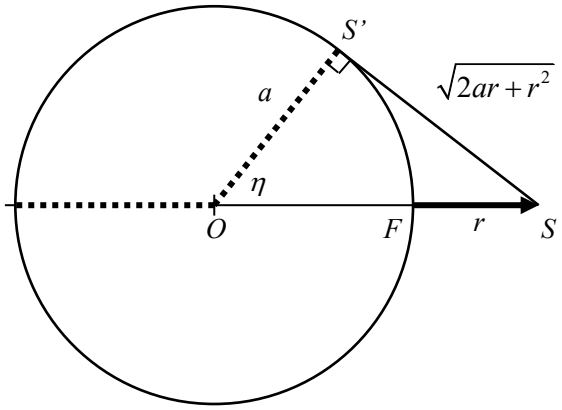

Figure 12 Linear Hyperbolic Model.

The initial condition depends on the problem. If we let $t = 0$ when r is zero (conic apex), motion is described as a simplified Eq. (54a),

$$\sqrt{\frac{\mu}{a}}\, t = a\tan\eta \; - a\ln\tan\left(\frac{\pi}{4} + \frac{\eta}{2}\right). \tag{55}$$

The time between two points in a real problem is obtained by subtracting one state represented by Eq. (55) from another, eliminating the constant of integration.

Dynamic Models

The steps for developing dynamic hyperbolic models are similar to those of the other orbits. A multiplier times the lines in the models above will yield vectors that are the square root of twice the energy values in the energy conservation equation. The multiplier in this case is $\left(\sec\eta\dot{\eta}\right)$. Differentiate Eq. (53) with respect to time and write

$$\dot{r} = ae\tan\eta\sec\eta\dot{\eta}\,. \tag{56}$$

and differentiating Eq. (54) with respect to time gives

$$\sqrt{\frac{\mu}{a}} = ae\sec^2\eta\dot{\eta} - a\sec\eta\dot{\eta} = r\sec\eta\dot{\eta} \tag{57}$$

The velocity normal to r is found by combining Eqs. (1) and (57),

$$\frac{\sqrt{\mu p}}{r} = \sqrt{ap}\sec\eta\dot{\eta} \tag{58}$$

A dynamic model for the linear hyperbolic trajectory is developed with $p = 0$. Then Eq. (58) is zero as there is no rotational component. Conservation of energy may be written as

$$\dot{r}^2 = \frac{2\mu}{r} + \frac{\mu}{a} \tag{59}$$

Radial velocity may be written as

$$\dot{r} = \sqrt{2ar + r^2}\sec\eta\dot{\eta} \tag{60}$$

The square root of twice the potential energy is found by combining Eqs. (59) and (60),

$$\sqrt{\frac{2\mu}{r}} = \sqrt{\dot{r}^2 - \frac{\mu}{a}} = \sqrt{2ar}\sec\eta\dot{\eta} \tag{61}$$

Equations (56), (59), and (61) give a model as shown in Figure 13.

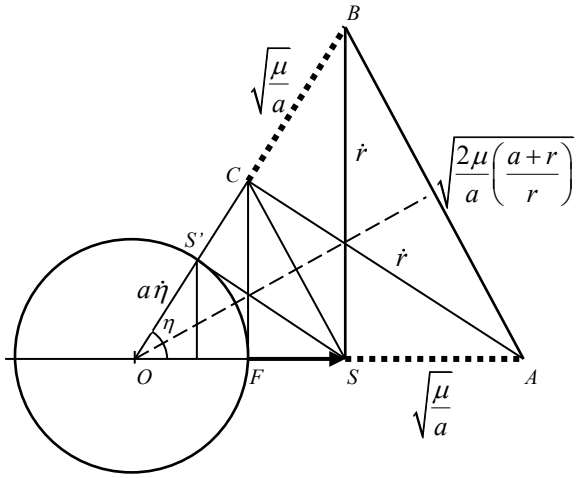

Figure 13 Dynamic Linear Hyperbolic Model.

Inspection shows that the vis viva equation must be modified to generate the appropriate triangle. Rearranging and adding μ/a to both sides gives

$$\dot{r}^2 + \frac{\mu}{a} = \frac{2\mu}{r} + \frac{2\mu}{a} = \frac{2\mu}{r}\left(\frac{a+r}{a}\right) \tag{62}$$

The lines in the model are a mirror image on either side of the line that bisects η, and triangles *ABS* and *ABC* represent Eq. (62). The triangle CFS (or CSS') is a reduced representation of Eq. (62). Each side is equal to the corresponding side of the *ABS* triangle multiplied by cos η.

General hyperbolic motion can be modeled in three dimensions in a manner like the general dynamic model for the ellipse. With the inclusion of the rotational component, Eq. (62) is written,

$$\dot{r}^2 + \frac{\mu p}{r^2} + \frac{\mu}{a} = \frac{2\mu}{r}\left(\frac{a+r}{a}\right) \cdot \tag{63}$$

The rotational term may be represented in the third dimension as in the elliptic model. Figure 14 shows the reduced general hyperbolic model that satisfies conservation of energy. The square root of twice the energy components multiplied by cos η are shown in the model as the *ABSS'* solid. The reduced model is shown for simplicity. The dotted lines in Figures 13 and 14 are constant and equal to $\sqrt{\mu/a}$.

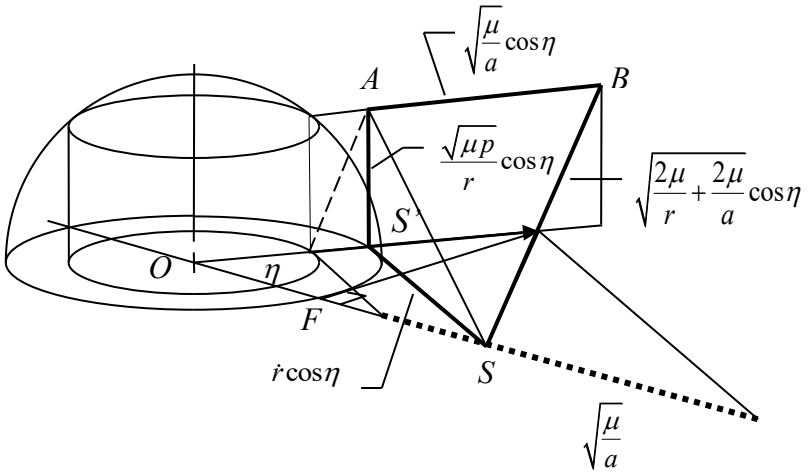

Figure 14 Reduced Dynamic General Hyperbolic Model.

Reconciling the Equation Differences

In computations, the classical time-displacement equation involving the hyperbolic anomaly agrees identically with the trigonometric equation derived above. The following relationship will show commonality:[6]

$$\cosh^{-1} x = \ln\left(x \pm \sqrt{x^2 - 1}\right) \cdot \tag{64}$$

This is compared to the hyperbolic anomaly expressed in the form[4]

$$\cosh H = \frac{e + \cos\theta}{1 + e\cos\theta} \cdot \tag{65}$$

With the substitution of Eq. (2) and $p = a(e^2 - 1)$, this may be written as

$$\cosh H = \frac{a + r}{ae} \cdot \tag{66}$$

Comparing Eq. (66) to Eq. (52) shows that $\cosh H$ is the reciprocal of $\cos\eta$. The term $\sinh H$ appears in the time-displacement equation. Thus, we have identical terms appearing in both the trigonometric equation derived and the classical equation. Both calculate the same answer. A further, more rigorous proof of equality is left to the reader.

Hyperbolic Excess Velocity

To show how hyperbolic models allow us to visualize the velocity as r approaches infinity, we can examine the limiting value of $\dot{r}$. As r approaches infinity and the potential energy approaches zero, kinetic energy approaches total energy.[2] Combining Eqs. (56) and (57), we can note that

$$\dot{r} = \frac{ae\tan\eta}{r}\sqrt{\frac{\mu}{a}} \tag{67}$$

Substitute Eq. (52) into Eq. (67) and rearrange to write

$$\dot{r} = \frac{e\sin\eta}{e-\cos\eta}\sqrt{\frac{\mu}{a}} \tag{68}$$

As η approaches its limit of $\pi/2$, radial velocity approaches the constant hyperbolic excess velocity expressed by

$$\dot{r} \to \sqrt{\frac{\mu}{a}} \tag{69}$$

The models show this result because the circles reduce to zero as η approaches $\pi/2$. As this occurs the lines in the models representing radial velocity coincide with the constant $\sqrt{\mu/a}$ lines.

Hyperbolic Transformation Equations

Transformation for hyperbolic orbits is found by equating Eq. (2) to Eq. (53) and substituting $p = a(e^2 - 1)$. Then

$$\frac{p}{1+e\cos\theta} = ae\sec\eta - a \tag{70}$$

which can be rearranged to give

$$\cos\theta = \frac{e\cos\eta - 1}{e-\cos\eta} \tag{71}$$

SUMMARY

The classical approach to two-body orbital time displacement analysis has its roots in Kepler's auxiliary circle construction and the introduction of the eccentric anomaly. The alternative method presented above begins with the fundamental forces acting on a satellite, separates terms that represent radial motion and motion normal to the radius, and follows with a sequence of integration steps. The same steps are followed for each type of orbit. Integration with respect to time produces equations and models, based on circles. This makes trigonometric relationships apparent for hyperbolic trajectories. Analyzing two-body motion with this approach leads to the following conclusions:

- All two-body orbital motion equations can be derived from a common set of force, power and conservation of energy equations.
- Displacement angles and models result naturally from the derivation for each trajectory type. The models show that there are suitable alternative coordinate systems to the classical perifocal system for modeling orbital motion.
- Each conic section has a rectilinear special case with eccentricity equal to one and the semi parameter equal to zero.
- Each case has a dynamic model that relates the terms in the energy conservation equation.
- General and linear parabolic motion can be expressed in algebraic equations.

REFERENCES

[1]May, D. H., Integrated Orbital Motion Equations with Conformance Models. Paper AIAA-99-4060 presented at the AIAA Guidance, Navigation, and Control Conference. Portland, OR. 1999.

[2]Bate, R. R., Mueller, D. D. and White, J. E., *Fundamentals of Astrodynamics*, Dover Publications, New York, 1971.

[3]Chobotov, V. A., *Orbital Mechanics,* American Institute of Aeronautics and Astronautics, Inc., Washington, DC, 1991.

[4]Vallado, D.A., *Fundamentals of Astrodynamics and Applications*, The McGraw-Hill Companies, Inc., New York, 1997.

[5]Greenwood, D. T., *Principles of Dynamics*, Prentice-Hall, Inc., Englewood Cliffs, NJ, 1965.

[6]Zwillinger, D., Standard Mathematical Tables and Formulae, 30th Edition, CRC Press, New York, 1996.